Bioconjugate Chemistry

Article

pubs.acs.org/bc

Poly(2-ethyl-2-oxazoline)–Doxorubicin Conjugate-Based Dual Endosomal pH-Sensitive Micelles with Enhanced Antitumor Efficacy

Jinwen Li, Yanxia Zhou, Chengwei Li, Dishi Wang, Yajie Gao, Chao Zhang, Lei Zhao, Yushu Li, Yan Liu,* and Xinru Li*

Department of Pharmaceutics, School of Pharmaceutical Sciences, Peking University, Beijing 100191, China

Supporting Information

ABSTRACT: Dual endosomal pH-sensitive micelles were designed and fabricated to deliver doxorubicin (DOX) for treating breast cancer based on a poly(2-ethyl-2-oxazoline) (PEOz)–DOX (PEOz–hyd–DOX) conjugate. PEOz–hyd–DOX was successfully synthesized by connecting DOX to PEOz via an acid cleavable hydrazone linker and self-assembled into nanosized micelles, which further physically encapsulated DOX. The conjugate and DOX-loaded conjugate micelles displayed faster release of DOX at pH 5.0 than at pH 7.4. This pH-dependent release behavior might assist the quick diffusion of DOX from acidic endosomes or lysosomes and the intracellular transfer into the nucleus after internalization, which was confirmed by confocal laser scanning microscopy images. As expected, PEOz–hyd–DOX conjugate and DOX-loaded conjugate micelles maintained cytotoxicity of DOX. In addition, the dual endosomal pH-sensitive micelles were found to substantially enhance antitumor efficacy and reduce side effects compared with free DOX. Therefore, PEOz–hyd–DOX conjugate-based micelles might be potential drug delivery vehicles of DOX for safe and effective breast cancer therapy.

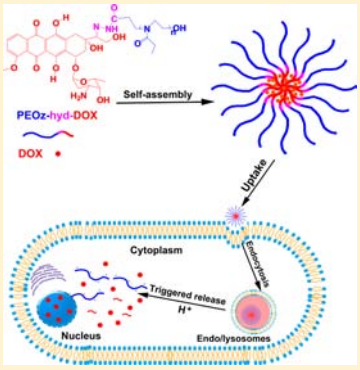

INTRODUCTION

Doxorubicin (DOX) is a potent anticancer agent that is effective against a wide range of solid tumors.[1] The mechanism of DOX to kill cancer cells is ensured via reactive oxygen species involving the quinone group in the anthracycline ring, and DOX can intercalate DNA to restrain topoisomerase.[2] However, the cytotoxic effect of DOX lacks specificity to cancer cells. For example, DOX can rapidly divide bone marrow cells and intestinal epithelial cells in short time and affect cardiac and hepatic tissues for a long time,[2] which greatly hampers its application to cancer therapy.

To overcome these limitations, macromolecular delivery systems such as liposomes,[3] polymeric micelles,[4] nanoparticles,[5] and polymersomes[6] have been widely investigated. Such delivery systems have demonstrated high accumulation in tumors via the enhanced permeation and retention (EPR) effect[7] and active cellular uptake.[8] Nevertheless, there are still some challenges to address such as premature release of drug in blood circulation. Recently, great attention has been paid to polymer–drug conjugates (PDCs) in which drugs were attached to polymers through acid cleavable covalent linkages such as hydrazone and *cis*-aconityl bonds, due to their high stability in normal physiological conditions and quick drug release in acidic environments such as the acidic endosomal or lysosomal compartments in tumor cells.[9] So far, there have been many PDCs investigated for DOX.[10−15] Some PDCs have entered into clinical trials, such as *N*-(2-hydroxypropyl) methacrylamide–DOX conjugate for the treatment of ovarian cancer.[14] Favorably, these PDCs reduced side effects of DOX while maintaining its antitumor efficacy.[15]

On the other hand, PDCs spontaneously form core–shell structured micelles taking advantage of their amphipathic nature in aqueous medium, thus enhancing the drug loading by physical encapsulation.[16] Notably, a great concern is that slow drug release of PDC micelles in tumor cells may result in lower level of free drug and thereby limit antitumor efficacy.[17] Even worse, maintaining a lower level of intracellular free drug for a long time may lead to occurrence of drug resistance for tumor cells. Consequently, to guarantee the delivery of PDCs to the tumor site and sufficient free drug concentration in tumor cells, PDC micelles are required to remain stable in blood circulation and rapidly release free drugs in tumor cells. This might be achieved by using PDC micelles with a triggered release mechanism that enables the micelles to release their cargos in response to the stimuli of tumor intracellular compartments, such as pH and enzymes.[18] pH-responsive polymeric micelles appeared to be the most attractive candidate because the internalized micelles experienced a pH gradient from 6.5 to 4.5 in endosomes or lysosomes in their intracellular trafficking pathway.[19,20] This stimuli can induce micelles to release encapsulated drugs in a specially controlled manner,[21] and PDCs with acid-sensitive linkages to quick release the conjugated drugs.[22,23]

In recent years, poly(2-ethyl-2-oxazoline) (PEOz) has gained much attention as a potential alternative to poly(ethylene glycol) (PEG) with higher water solubility, better flexibility, and

Received: October 14, 2014
Revised: December 12, 2014
Published: December 15, 2014

DOI: 10.1021/bc5004718
Bioconjugate Chem. 2015, 26, 110−119

lower toxicity.[24−27] Additionally, PEOz can be synthesized easily by the living cationic ring-opening polymerization of 2-ethyl-2-oxazoline and has been approved by the US Food and Drug Administration as a food additive.[28] More significantly, PEOz has a favorable pK_a[29] and can be ionized at endosomal or lysosomal pH.[30] Our previous work and other reports demonstrated that this property of PEOz promoted the release of drugs from micelles in which PEOz composed the outer shell at the acidic endocytic pH.[29,31]

In order to integrate the merits of PDC for reduced drug release in circulation and pH-sensitive micelles for enhanced accumulation in tumor site and quick drug release in tumor cells, we fabricated dual endosomal pH-sensitive PDC micelles to encapsulate DOX based on the conjugate of DOX with PEOz via hydrazone linkers (denoted as PEOz−hyd−DOX). Schematic illustrations depicting the formation of pH-sensitive micelles and the intracellular trafficking are presented in Figure 1. We hypothesized that the micelles would be an effective

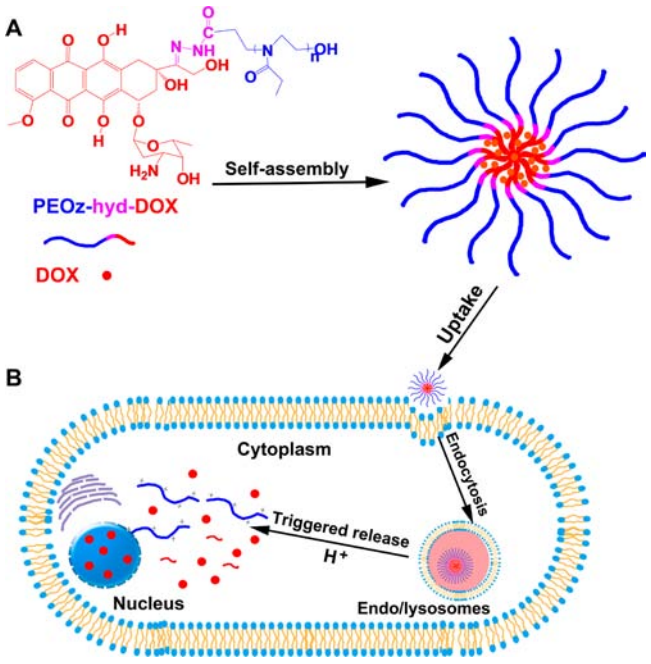

Figure 1. Schematic illustrations of the formation of dual endosomal pH-sensitive micelles based on PEOz−hyd−DOX (A) and their endocytosis and pH-triggered release (B).

delivery system for DOX by relying on EPR effect and controlled drug release by the pH gradient subjected on micelles in their endocytic pathway. Hence, the physicochemical properties, pH-dependent drug release, *in vitro* cytotoxicity against MCF-7 cells, and cellular uptake, as well as *in vivo* antitumor efficacy, were evaluated in detail.

RESULTS

Synthesis and Characterization of PEOz−hyd−DOX Conjugate. The successful synthesis of PEOz-COOH (Figure 2A) was confirmed by ^{1}H NMR spectrum (Figure 3A). The sharp peaks at 3.39 and 2.36 ppm were attributed to methylene protons in main and side chains, respectively. The peak at 1.01 ppm was assigned to methyl protons in side chains. These were in good agreement with our previous report.[28] In FTIR spectra of PEOz-COOH (Figure 3F, trace a), the band at 1652 cm^{-1} was characteristic for the carbonyl vibration of the amide

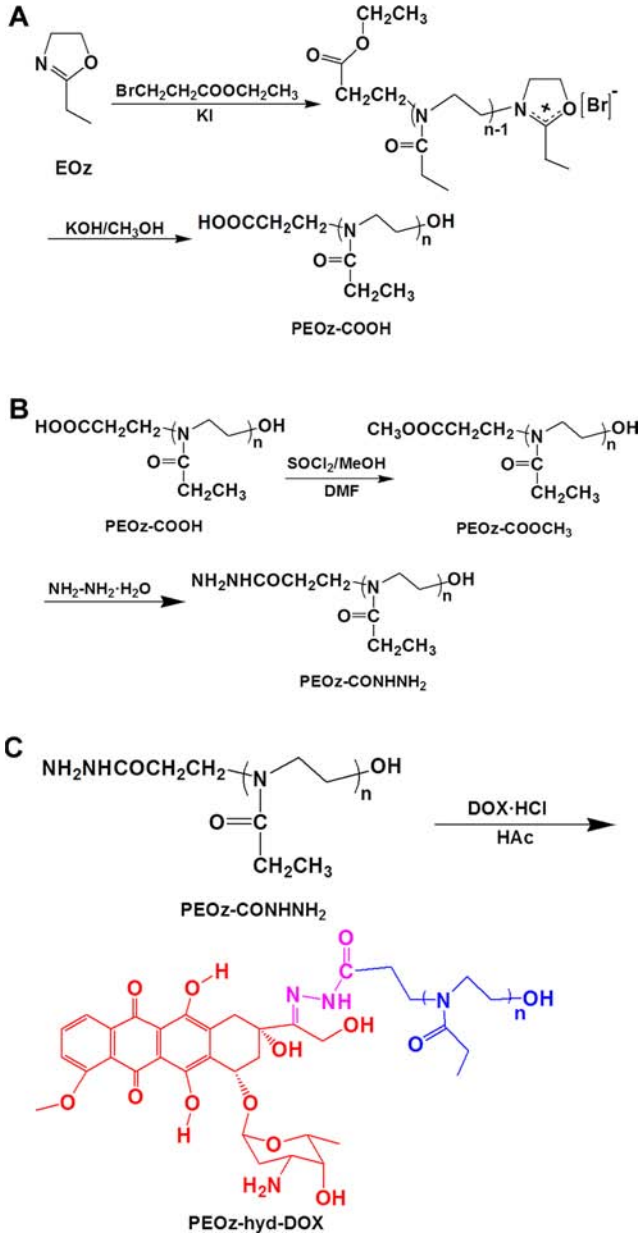

Figure 2. Synthesis routes of PEOz-COOH (A), PEOz-CONHNH$_2$ (B), and PEOz−hyd−DOX conjugate (C).

groups.[30] The band at 1736 cm^{-1} was attributed to the characteristic carbonyl absorption of the terminal carboxyl group. The number-average molecular weight of the synthesized PEOz-COOH was 2610 g/mol with 1.48 polydispersity index (PDI) determined by GPC (Figure 3E), suggesting that the obtained PEOz-COOH had well-controlled M_n and narrow distribution of molecular weight. Further, the pK_a of PEOz-COOH was determined to be 6.19 ± 0.02, obtained from acid/base titration profiles (Figure S1, Supporting Information).

Afterward, PEOz-COOH was first activated by treatment with thionyl chloride, esterified with CH_3OH, and then reacted with hydrazine hydrate (Figure 2B). The linkage of PEOz-COOH with hydrazine hydrate was supported by thin layer chromatograms (TLC) of the product compared with PEOz-COOH and hydrazine hydrate (Figure 3D1).

Finally, PEOz−hyd−DOX was synthesized by conjugation of DOX to the pendant hydrazide group of PEOz-CONHNH$_2$

DOI: 10.1021/bc5004718
Bioconjugate Chem. 2015, 26, 110−119

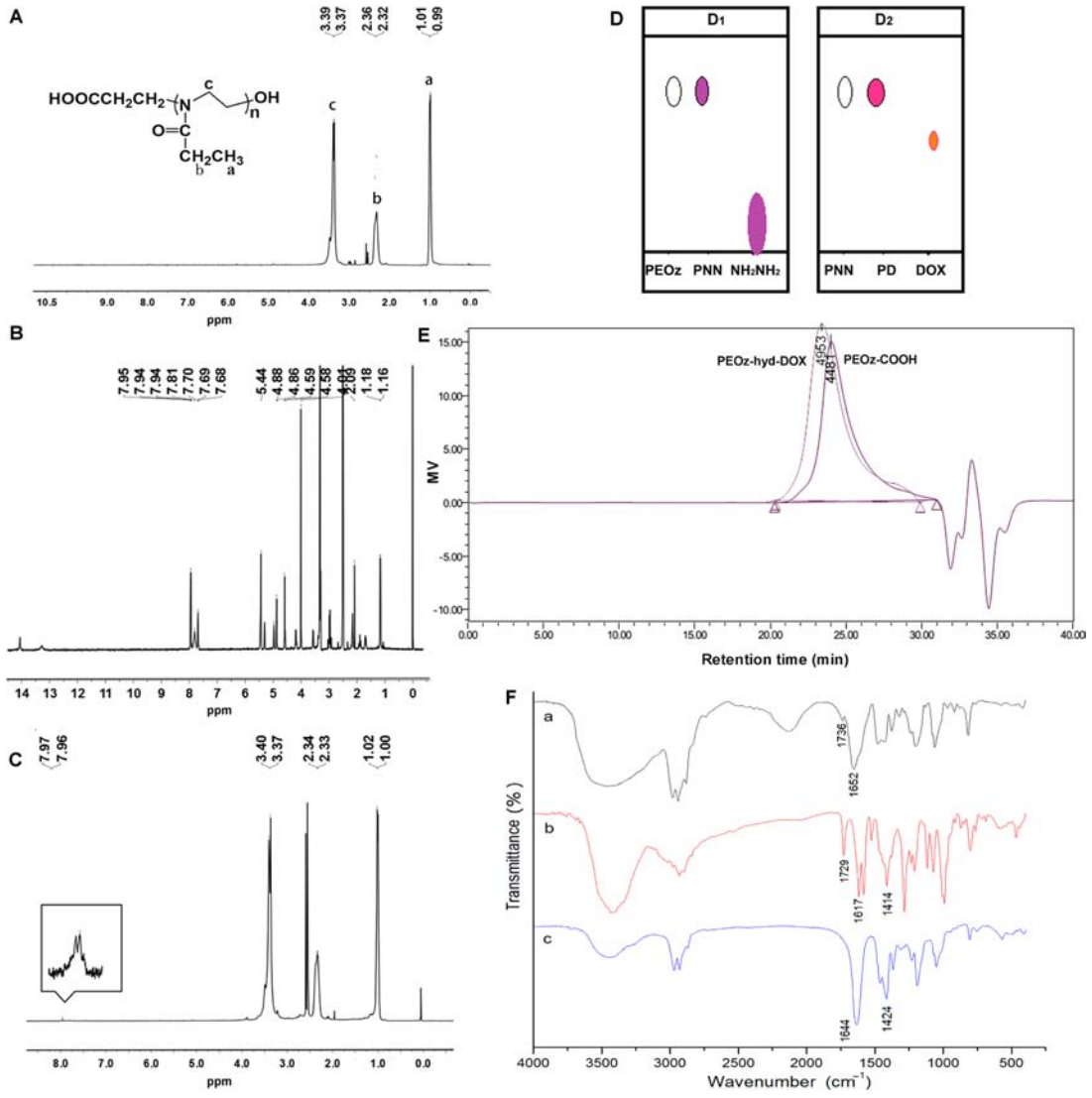

Figure 3. ^{1}H NMR spectra of PEOz-COOH (A), DOX (B), and PEOz−hyd−DOX (C) in DMSO-d_6. (D) Thin layer chromatograms of PEOz-COOH (PEOz), PEOz-CONHNH$_2$ (PNN), PEOz−hyd−DOX (PD), $NH_2NH_2{\cdot}H_2O$ (NH_2NH_2), and DOX. PEOz-CONHNH$_2$ and $NH_2NH_2{\cdot}H_2O$ were developed to be purple spots by ninhydrin; PEOz−hyd−DOX and DOX showed fluorescence under 365 nm UV lamp. (E) The gel permeation chromatograms of PEOz-COOH and PEOz−hyd−DOX. (F) FTIR spectra of PEOz-COOH (a), DOX (b), and PEOz−hyd−DOX (c).

through the formation of an acid-sensitive hydrazone bond (Figure 2C). The conjugation was confirmed by ^{1}H NMR spectrum (Figure 3C) and TLC (Figure 3D2). The peaks at 7.96 and 7.97 ppm were assigned to the phenyl protons of DOX, which were also observed in Figure 3B, and the characteristic peaks corresponding to PEOz-COOH (1.10, 2.39, and 3.45 ppm) indicated the successful synthesis of the conjugate. In addition, TLC suggested the formation of the desired product (Figure 3D2), in which the dull-red fluorescence spot, being similar to that of DOX, of PEOz−hyd−DOX was found at the same site of PEOz-CONHNH$_2$, whereas this phenomenon was not found for PEOz-CONHNH$_2$. The conjugation was further supported by GPC (Figure 3E). FTIR spectra were also used to prove the successful conjugation of DOX with PEOz (Figure 3F). In spectra of DOX (Figure 3F, trace b), the band at 1617 cm^{-1} was the characteristic carbonyl absorption of anthracene ring. A narrow peak appearing at 1729 cm^{-1} was attributed to the stretching vibration of the reactive carbonyl group. A strong peak at 1414 cm^{-1} resulted from N−H vibration. As for the spectra of PEOz−hyd−DOX (Figure 3F, trace c), the band at 1644 cm^{-1} resulted from the carbonyl vibration of the amide groups on PEOz, whereas the carbonyl absorption peak at 1736 cm^{-1} of the terminal carboxyl group on PEOz disappeared. Likewise, the carbonyl absorption peak at 1729 cm^{-1} of the reactive carbonyl group on DOX was not found due to the formation of the hydrazone bond, while a strong peak at 1424 cm^{-1} resulting from N−H vibration was assigned to the presence of DOX in the conjugate backbone. In addition, the peak at 1617 cm^{-1} of carbonyl absorption of the anthracene ring on DOX might be overlain by the peak at 1644 cm^{-1} of the carbonyl vibration of the amide groups on PEOz.

To demonstrate the cleavage of hydrazone bonds in the acidic environment, PEOz−hyd−DOX conjugate was incubated in either phosphate buffer solution (PBS, pH 7.4, 10 mmol/L) or acetate buffer solution (ABS, pH 5.0, 10 mmol/L), and the amount of the released DOX at different times was measured by HPLC. As shown in Figure 4A, the accumulative release of DOX from PEOz−hyd−DOX conjugate increased dramatically at pH 5.0 compared with that at pH 7.4.

DOI: 10.1021/bc5004718
Bioconjugate Chem. 2015, 26, 110−119

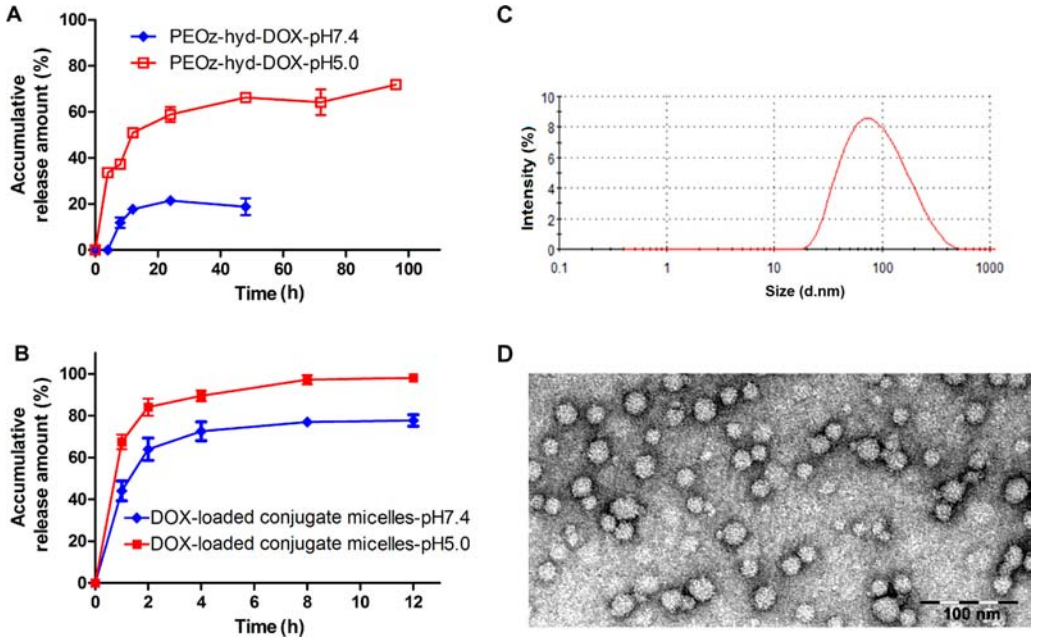

Figure 4. *In vitro* release profiles of DOX from PEOz−hyd−DOX conjugate (A) and DOX-loaded conjugate micelles (B) at different pH values at 37 °C (n = 3). Size distribution (C) and transmission electron microscope images (D) of DOX-loaded conjugate micelles.

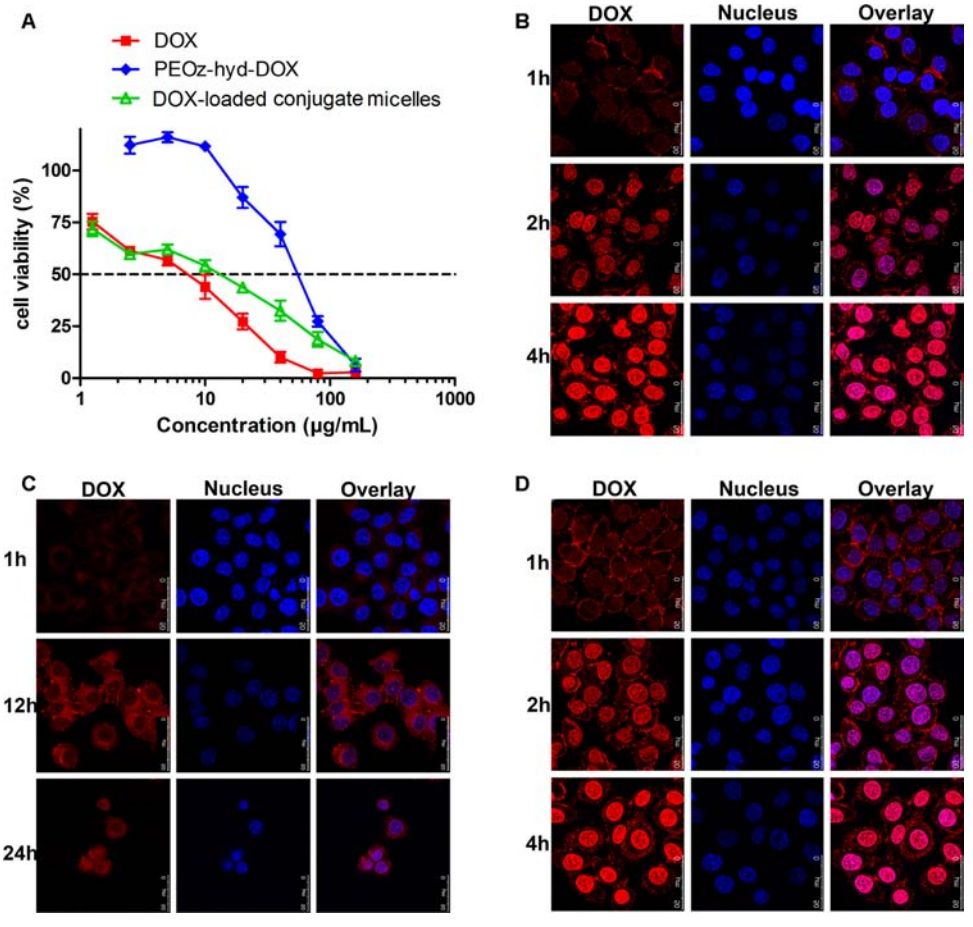

Figure 5. (A) DOX concentration-dependent effect of different DOX formulations on the viability of MCF-7 cells following incubation for 24 h at 37 °C (n = 4). Confocal laser scanning microscopy images of MCF-7 cells incubated with free DOX (B), PEOz−hyd−DOX conjugate (C), and DOX-loaded conjugate micelles (D) at 37 °C for different times. The final DOX concentration in each formulation was 10 μg/mL. Cell nuclei were stained blue with Hoechst 33258 and overlaid with red fluorescence images of DOX.

DOI: 10.1021/bc5004718
Bioconjugate Chem. 2015, 26, 110−119

Specifically, about 34% of DOX was released from the conjugate within the first 4 h, while about 72% of DOX was released after 96 h. However, no DOX was released from PEOz−hyd−DOX conjugate over the course of the first 4 h at pH 7.4, and only about 21% of DOX was released within 24 h. Afterward, the release profile reached a plateau. These results indicated the acid sensitivity of the PEOz−hyd−DOX conjugate. Nevertheless, it should be noted that only 72% of DOX was released from PEOz−hyd−DOX conjugate at pH 5.0 within 96 h, possibly due to the insufficient release time and the instability of DOX in acidic aqueous solution. The acidic hydrolysis of DOX to doxorubicinone, which is related to time and temperature,[32] might cause the determined content of DOX in release medium to be lower than that of the actually released DOX.

Preparation and Characterization of Micelles. PEOz−hyd−DOX conjugate could self-assemble into micelles in which DOX composed the inner core and PEOz composed the outer shell, which was confirmed by DLS measurement and TEM observation. The average diameter of DOX-loaded conjugate micelles was about 65 nm (Figure 4C) with 0.28 PDI. TEM images showed that DOX-loaded conjugate micelles had a well-defined spherical shape and uniform size (Figure 4D). Noticeably, it appeared that the size of DOX-loaded conjugate micelles measured by TEM was smaller than that determined by DLS, which might be due to the shrinkage of the micelles on the grid surface during drying and staining of the TEM specimen and the swelling or stretching of the shell-forming PEOz chain in the hydrated state of the micelles for DLS measurement.[33,34]

The loading content of DOX-loaded conjugate micelles including encapsulated and conjugated DOX was 6.8% ± 0.1%, and the encapsulation efficiency of the micelles was 86.9% ± 1.8%.

In addition, stability is a very important property of micelles to understand *in vitro* drug uptake and *in vivo* absorption; the size of DOX-loaded conjugate micelles in PBS and cell culture medium was therefore monitored at different times at room temperature. Within 12 h, DOX-loaded conjugate micelles did not show a remarkable change in size ranging from 61 to 63 nm in PBS and 74 to 76 nm in cell culture medium, indicating that DOX-loaded conjugate micelles had considerably high thermodynamic stability without aggregation.

***In Vitro* pH-Dependent Release of DOX from Micelles.** The *in vitro* release of DOX from DOX-loaded conjugate micelles at 37 °C was evaluated over 12 h using a dialysis method at pH 7.4 that mimics the blood environment and in the environment under endosome/lysosome mimetic circumstances (pH 5.0). As shown in Figure 4B, DOX-loaded conjugate micelles showed a remarkably slower release at pH 7.4 during the whole experiment period compared with that at pH 5.0. Specifically, at pH 7.4, about 65% of DOX was released from DOX-loaded conjugate micelles within the first 4 h, and then the DOX release profile reached a plateau. In comparison, the release of DOX from DOX-loaded conjugate micelles was profoundly accelerated at pH 5.0; about 90% of DOX released within 4 h and almost 98% of DOX leaked after 12 h. These results suggested that DOX-loaded conjugate micelles were sensitive to endosomal/lysosomal pH.

***In Vitro* Cytotoxicity Assay.** The *in vitro* cytotoxicity of various DOX formulations against MCF-7 cells was evaluated using SRB assay. Apparent cell growth inhibition was observed in a concentration- and formulation-dependent pattern (Figure 5A). Noticeably, free DOX (IC_{50} = 5.38 ± 0.71 μg/mL) exhibited the highest cytotoxicity owing to its easier internalization and accumulation in cells at high level.[35] PEOz−hyd−DOX conjugate (IC_{50} = 51.35 ± 2.53 μg/mL) lowered the cytotoxicity of DOX, whereas the encapsulation of DOX into the conjugate micelles (IC_{50} = 8.58 ± 1.36 μg/mL) resulted in obvious increase in the cytotoxicity of DOX. These results demonstrated that both PEOz−hyd−DOX conjugate and DOX-loaded conjugate micelles manifested cell growth inhibitory activity against MCF-7 cancer cells, indicating hydrolysis of the hydrazone bond in PEOz−hyd−DOX and release of DOX physically entrapped in conjugate micelles, respectively.

Cellular Uptake and Intracellular Distribution Study. Confocal laser scanning microscope (CLSM) was used to visually observe the cellular uptake and subcellular distribution of various DOX formulations in MCF-7 cells at an equivalent 10 μg/mL of DOX, respectively. Figure 5B−D presents the intracellular accumulation and distribution of various DOX formulations. As seen from Figure 5B, MCF-7 cells treated with free DOX for 1 h presented a strong DOX fluorescence in nucleus, and the red fluorescence intensity in nucleus increased with increased incubation time. After 4 h incubation, the free DOX was mainly distributed within the nucleus with overlay of pink fluorescence. In comparison, intense red fluorescence of PEOz−hyd−DOX conjugate was observed around the nucleus at 1 h resulting in a broad intracellular distribution in the cytoplasm, and no red fluorescence was observed in the nucleus (Figure 5C), showing that the conjugate was easily and quickly internalized into cells. After 12 h treatment, weak red fluorescence was observed in the nucleus and a large portion of the PEOz−hyd−DOX conjugate was mainly located in the cytoplasm. Although the cells became unhealthy at 24 h, it was obvious that the distribution of the conjugated DOX in the nucleus increased. These results were in good agreement with the pH-responsive cleavage behavior of PEOz−hyd−DOX conjugate and indicated that the conjugation of DOX with PEOz made its intracellular delivery kinetics different. As for DOX-loaded conjugate micelles in which there existed DOX physically entrapped in micelles and DOX chemically bound to polymer, the time-dependent cellular uptake and intracellular distribution of the micelles (Figure 5D) were similar to those of free DOX (Figure 5B) and different from those of the conjugate (Figure 5C), evidencing that the conjugate micelles were rapidly internalized into cells, which was judging by the red fluorescence at 1 h (Figure 5D). The images showed an intense red fluorescence in both the nucleus and the cytoplasm at 1 h, suggesting that DOX physically entrapped in the conjugate micelles released more rapidly from the micelles compared with DOX chemically bound to polymer, and then readily escaped from endosomes or lysosomes and entered into the nucleus, which might be attributed to the pH-responsibility of the conjugate micelles.

***In Vivo* Antitumor Efficacy.** The *in vivo* antitumor efficacy of various DOX formulations was evaluated in MCF-7 xenograft-bearing athymic nude mice. Figure 6A presents the tumor growth curves. Overall, the tumor volume of animals treated with various DOX formulations reduced continuously compared with the saline group after the second treatment, implying that all DOX formulations were effective to some extent in inhibiting the growth of MCF-7 xenografts. Inspiringly, DOX-loaded conjugate micelles were found to be more effective than either free DOX or PEOz−hyd−DOX

DOI: 10.1021/bc5004718
Bioconjugate Chem. 2015, 26, 110−119

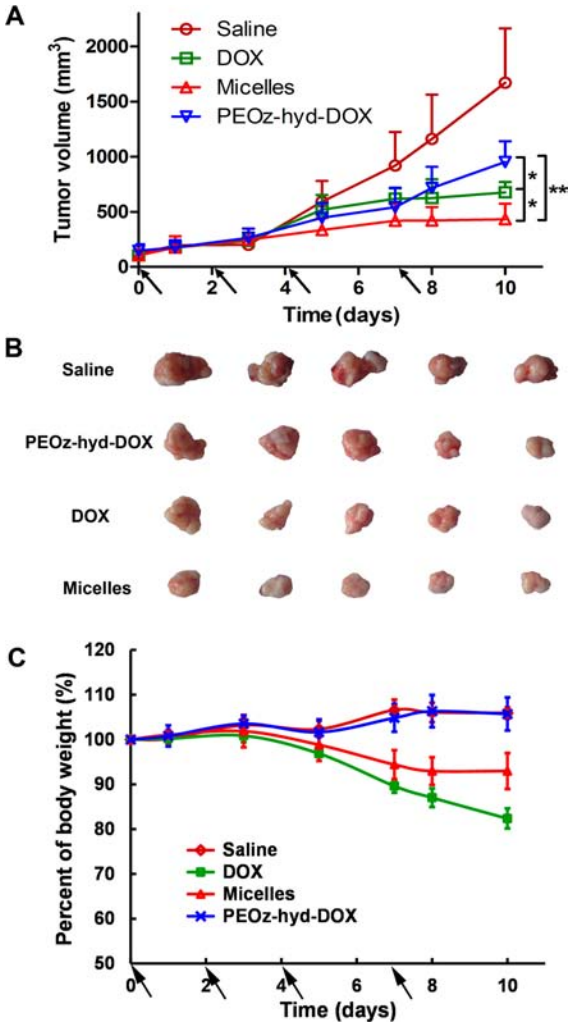

Figure 6. *In vivo* antitumor efficacy and systemic toxicity of free DOX, PEOz–hyd–DOX conjugate, and DOX-loaded conjugate micelles injected into MCF-7 tumor bearing athymic nude mice at DOX dose of 5 mg/kg (n = 5). (A) Changes of tumor volume after treatments. The arrows indicated injection time points. (B) MCF-7 tumor mass from each treatment group excised on day 10 after treatments. (C) Body weight changes after treatments. *p < 0.05 and **p < 0.01.

conjugate at the 10-day time point after treatment and achieved statistical significance compared with either DOX-treated group (p < 0.05) or PEOz–hyd–DOX conjugate-treated group (p < 0.01). In addition, free DOX showed a superior efficacy than PEOz–hyd–DOX conjugate (p < 0.05). These results were also supported by the images of the tumor mass excised on day 10 after treatments from the xenograft mice (Figure 6B). The tumor growth inhibition after 10-day treatment for free DOX, PEOz–hyd–DOX conjugate, and DOX-loaded conjugate micelles was calculated to be 62.3%, 45.5%, and 72.4%, respectively.

The body weight of the mice was also monitored every 2 days following administration of various DOX formulations to evaluate their side effects during the experimental period (Figure 6C). There was no significant change in body weight for saline, PEOz–hyd–DOX conjugate, and DOX-loaded conjugate micelle groups of mice during the whole experimental period, implying their better drug tolerability. Further, the body weight for PEOz–hyd–DOX conjugate and DOX-loaded conjugate micelles groups maintained normal fluctuation, suggesting a low systemic toxicity. In contrast, treatment with free DOX produced obvious side effects such as weight loss of more than 20% in mice at the end of the experimental period. These results indicated that both the conjugation of DOX and the encapsulation of DOX in the micelles remarkably reduced the exposure of normal tissues to DOX and thus decreased the toxicity of DOX.

DISCUSSION

Conjugation of hydrophilic polymers with hydrophobic anticancer drugs to form PDC has been proven to be a viable strategy for reducing side effects;[36] thus there has been growing interests in design, development, and utilization of PDCs for drug delivery. In this study, a novel, water-soluble, and pH-responsive polymer PEOz was first attempted to conjugate with DOX via hydrazone bonds to generate PEOz–hyd–DOX conjugate, and the feasibility of dual endosomal pH-responsive DOX-loaded PEOz–hyd–DOX micelle delivery system with enhanced antitumor activity and substantially reduced systemic toxicities was explored.

PEOz containing one pendant carboxyl group was successfully synthesized by cationic ring-opening polymerization of EOz initiated by ethyl 3-bromopropionate and terminated by methanolic KOH.[37] By controlling the molar ratio of initiator (ethyl 3-bromopropionate) to monomer (EOz), PEOz-COOH with the desired molecular weight could be obtained. Notably, moisture has a significant effect on achieving high molecular weight polymers. Polymerization in nondrying solvent or with nondrying monomer, initiator, and terminator would only generate short polymer chains due to the termination of the chain elongation in the presence of water in the reaction system.[38,39] Therefore, reflux and subsequent distillation of all agents over calcium hydride was performed under an atmosphere of high purity nitrogen before the reaction occurs, and high purity nitrogen was bubbled through the reaction mixture to exclude air during the reaction. Additionally, the conjugation of DOX to PEOz-$CONHNH_2$ through the formation of pH-sensitive hydrazone bond, being confirmed by the acid-sensitive release of DOX from the obtained conjugate (Figure 4A), must be free from acids and strictly anhydrous due to the instability of hydrazone bond under acidic water environment.

The most striking observation of this study was the maintenance of antitumor activity along with greatly reduced side effects of DOX after conjugating with the polymer (Figure 6). Furthermore, the release of the conjugated DOX from PEOz–hyd–DOX conjugate was accelerated at endosomal/lysosomal pH (Figure 4A), benefiting from the pH-cleavable hydrazone bonds that connected DOX to PEOz. Unfortunately, the drug loading content of PEOz–hyd–DOX conjugate was not satisfactory. An alternative strategy to overcome this shortcoming is to physically encapsulate DOX in the micelles formed by the conjugate. This is an ingenious approach to enhance the drug loading content through increase of the chemical compatibility between the encapsulated drug and the micelle core and thereby intracellular delivery of drug.[16] Favorably, PEOz–hyd–DOX conjugate possessing amphiphilic nature with PEOz as hydrophilic segment and DOX as hydrophobic segment could self-assemble into nanosized micelles (Figure 4C,D); the loading content of DOX was enhanced up to 3-fold higher than the conjugate. Nevertheless, the loading content of micelles prepared using the optimal processing technique was only about 7%, which might be

DOI: 10.1021/bc5004718
Bioconjugate Chem. 2015, 26, 110–119

attributed to the short chain of DOX forming the inner core of micelles and its branched chain structure. Further studies for additional increase of the loading content by inserting a hydrophobic segment between PEOz and DOX to enlarge the inner core of micelles or conjugating several DOX molecules to one polymer chain are in progress. What's more, these nanosized micelles might be beneficial for a passive targeting delivery of drugs to tumors since they were small enough to penetrate through the leaky tumor vasculature via EPR effect,[39] while reducing reticuloendothelial system mediated clearance, and big enough to avoid renal filtration.[40] As expected, the DOX-loaded conjugate micelles distinguished endocytic pH from physiological pH by accelerating drug release (Figure 4B). This pH-triggered quick drug release was assigned to pH-sensitive hydrazone linker and, especially, the peculiar structure of PEOz located in the outer shell of the micelles. When the pH value in the environment was lower than the pK_a of PEOz, the amide groups of PEOz were ionized, leading to electrostatic repulsion between PEOz chains, which may induce the loosening of the micelle structure.[30] In addition, increased hydrophilicity of DOX in acid conditions also resulted in a rapid release of DOX.[40] This endocytic pH-triggered release behavior of DOX-loaded conjugate micelles facilitated the quick diffusion of drug from the acidic endosomes or lysosomes and intracellular transfer, which was supported by subcellular distribution (Figure 5C), and thereby remarkably enhanced the intracellular free drug concentration in a short time once the micelles were internalized via endocytosis,[17] being beneficial to kill tumor cells and shrink tumors[31,41,42] and possibly deterring the occurrence of drug resistance for tumor cells. This hypothesis was further confirmed in the present study by enhanced antitumor efficacy (Figure 6A,B) and reduced side effects (Figure 6C).

It was noteworthy that no correlation was found between *in vitro* antitumor effect (Figure 5A) and *in vivo* antitumor efficacy (Figure 6A) for various DOX formulations. Such divergence might be a consequence of the difference of cellular internalization rate, drug release rate inside the cells, pharmacokinetics, and biodistribution. Free DOX is a small molecule that can easily internalized into cells via passive diffusion,[35] thus resulting in quick cellular uptake (Figure 5B) and thereby the highest cytotoxic effect (Figure 5A), which was also supported by previous reports.[12,21] The superior *in vitro* cytotoxicity of DOX-loaded conjugate micelles to PEOz−hyd−DOX conjugate might be explained by the faster release of DOX physically entrapped in the micelles (Figure 4). The released DOX could rapidly escape from endosomes or lysosomes and then transfer to the nucleus through a diffusion mechanism (Figure 5C). Consequently, fast delivery of DOX into the nucleus could be achieved by using the dual pH-sensitive drug release property of the conjugate micelles. In addition, the feature of pharmacokinetics and biodistribution of various DOX formulations would have an impact on their antitumor efficacy.[21] Thus, the better antitumor effect of the conjugate micelles might be assumed to be a result of their long blood circulation, passive tumor targeting effect,[8] and dual endosomal pH-sensitivity. Overall, the design concept in this study might provide a facile strategy toward the design and fabrication of nanocarriers for safe and effective cancer therapy.

CONCLUSION

Dual endosomal pH-responsive conjugate micelles composed of a PEOz shell and DOX core via an acid cleavable hydrazone linkage was developed. PEOz−hyd−DOX retained the DOX biological activity to some extent, which was assigned to an effective release of DOX from the conjugate following intracellular delivery. In addition, PEOz−hyd−DOX readily self-assembled into nanosized micelles with narrow distribution. More importantly, DOX-loaded PEOz−hyd−DOX micelles demonstrated more effective antitumor effect *in vivo* over free DOX with a low systemic toxicity.

EXPERIMENTAL PROCEDURES

Materials and Animals. 2-Ethyl-2-oxazoline (EOz) was supplied by Sigma-Aldrich (St Louis, MO, USA). Potassium iodide (KI) and ethyl 3-bromopropionate were purchased from Aladdin Co., Ltd. (Shanghai, China). Hydrazine hydrate and thionyl chloride ($SOCl_2$) were purchased from Ouhechem Technology Co., Ltd. (Beijing, China). Doxorubicin hydrochloride (DOX·HCl) was provided by Haizheng Pharmacy (Zhejiang, China). Sulforhodamine B (SRB) sodium salt was purchased from Sigma-Aldrich (St Louis, MO, USA). RPMI-1640 cell culture medium, penicillin−streptomycin solution, fetal bovine serum (FBS), trypsin-EDTA, 25 and 75 cm^2 plastic culture flasks, and 24-well and 96-well tissue culture plates were supplied by M&C Gene Technology (Beijing, China). Hoechst 33258, 4% paraformaldehyde solution, and glycerin jelly were obtained from Biodee Biotechnology Co., Ltd. (Beijing, China). All other reagents and chemicals were of analytical grade or better.

Normal female athymic nude mice (4−5 weeks old) weighing 20−25 g were obtained from Animals Center of Peking University Health Science Center. They were kept in self-contained filter-top plastic cages and raised under standard conditions with free access to sterile food and water. All care and handling of animals were performed with the approval of Institutional Authority for Laboratory Animal Care of Peking University.

Synthesis and Characterization of End-Group-Carboxylated PEOz (PEOz-COOH). PEOz-COOH was synthesized by cationic ring-opening polymerization of 2-ethyl-2-oxazoline (20 mL) using ethyl 3-bromopropionate (0.5 g) and KI (molar ratio of 1:1.1) as initiators for 24 h in acetonitrile (70 mL) under nitrogen atmosphere and reflux conditions (Figure 2A).[31,37] After this period, the mixture was cooled to room temperature, and the reaction was quenched by adding 10 equiv of methanolic KOH followed by reflux overnight with stirring.[28] Then the resultant mixture was filtered through a Sabouraud funnel 3 times to remove salts. The solvent was then removed from the filtrate by rotary evaporation. The crude product was dissolved in deionized water and dialyzed with a dialysis membrane (MWCO 1000, Spectrum Laboratories) against deionized water for 24 h. The dialysis solution was subsequently lyophilized to obtain white solid of PEOz-COOH.

The product was characterized by ^{1}H NMR, FTIR, and gel permeation chromatography (GPC). The obtained product was dissolved in DMSO-d_6, and then the ^{1}H NMR spectrum was recorded on a Bruker MSL2300 spectrometer (400 MHz, Germany) using tetramethylsilane (TMS) as an internal reference at room temperature. FTIR spectra were obtained on a Nicolet Nexus 470 spectrometer using KBr as the sample holder. The molecular weight and molecular weight distribution were determined by gel permeation chromatography (GPC, Waters 1515) equipped with a refractive index detector (Waters 2414) and column (Styragel HT4-HT3-HT2, 10 μm, 7.8 mm ×

DOI: 10.1021/bc5004718
Bioconjugate Chem. 2015, 26, 110−119

300 mm) using polystyrene as standard. Tetrahydrofuran was used as eluent at 35 °C with a flow rate of 1.0 mL/min.

Synthesis and Characterization of End-Group-Hydrazided PEOz (PEOz-CONHNH$_2$). PEOz-CONHNH$_2$ was synthesized through two steps (Figure 2B) according to previous reports with a little modification.[43,44] First, PEOz-COOH (8 mmol, 20 g) dried by water segregator was dissolved in anhydrous methanol (100 mL), and then thionyl chloride (80 mmol, 5.7 mL) was added dropwise at 0−5 °C (salt−ice bath), followed by addition of a few drops of DMF. The resultant mixture was stirred for 2 h in a salt−ice bath, refluxed overnight in an oil bath with stirring, and concentrated by rotary evaporation. The product PEOz-COOCH$_3$ was recovered by precipitating in anhydrous ether and dried under vacuum for several hours. Second, to a solution of the resultant PEOz-COOCH$_3$ in methanol, a solution of hydrazine hydrate in methanol (1 mL/10 mL) was added slowly at a molar ratio of 20:1 to PEOz-COOCH$_3$. The resulting reaction mixture was stirred at room temperature for 24 h and dialyzed against deionized water for 24 h followed by lyophilization. Thin layer chromatography (TLC) was selected to confirm the successful synthesis of PEOz-CONHNH$_2$.

Synthesis and Characterization of PEOz−hyd−DOX Conjugate. The conjugation of DOX to PEOz-CONHNH$_2$ was achieved by formation of a hydrazone between the ketone of DOX and the hydrazide of PEOz-CONHNH$_2$ (Figure 2C) according to the previous report with a little modification.[45] Briefly, PEOz-CONHNH$_2$, DOX·HCl, and acetic acid at a molar ratio of 1:0.4:4 were dissolved in anhydrous DMSO and reacted for 24 h in the dark under stirring at room temperature. After the reaction finished, the red powdery PEOz−hyd−DOX conjugates were obtained by precipitating in anhydrous ether, drying under vacuum, purifying by Sephadex G25 column with distilled water (pH 7.8, adjusted with diluted sodium hydroxide aqueous solution) as eluent, and lyophilizing. The whole procedure was performed in the dark. Conjugation was confirmed by TLC, ^{1}H NMR, FTIR, and GPC.

The acid degradation of PEOz−hyd−DOX was conducted using a dialysis-bag diffusion technique. Briefly, 1.80 mg of lyophilized powder of PEOz−hyd−DOX (containing 0.038 mg of DOX) was dissolved in 1 mL of deionized water and then transferred into a dialysis bag (MWCO 1000). The sealed dialysis bag was then immersed into 30 mL of ABS (pH 5.0, 10 mmol/L) and PBS (pH 7.4, 10 mmol/L) at 37 °C in the dark with continuously shaking at 100 rpm. At predetermined time intervals, 1 mL of the media was taken out and immediately replaced with 1 mL of fresh media. The withdrawn media was analyzed with a Shimadzu series HPLC system (Shimadzu LC-10AT, Kyoto, Japan) equipped with a UV detector (Shimadzu SPD-10A) and reversed phase column (ODS C18, 5 μm, 4.6 mm × 250 mm, Dikma, China). Water (containing 0.28% SDS and 0.14% phosphoric acid)/acetonitrile/methanol = 50:70:6 (v/v/v) was used as the mobile phase at 30 °C with a flow rate of 1.0 mL/min. The detection wavelength was set at 233 nm. The content of DOX in PEOz−hyd−DOX solution in dialysis bag was considered to be 100%.

Determination of pK_a of PEOz-COOH. Acid dissociation constant (pK_a) of PEOz-COOH was determined by acid−base titration with sodium hydroxide.[42] Briefly, PEOz-COOH was dissolved in hydrochloric acid (0.01 mol/L) to reach a concentration of 10 mg/mL. Then the solution was titrated against sodium hydroxide aqueous solution (0.02 mol/L) under stirring, and the pH value was monitored using a pH meter during titration. The pK_a of PEOz-COOH corresponds to the pH value at which the ionization degree is 0.5.

Preparation of DOX-Loaded PEOz−hyd−DOX Conjugate Micelles. DOX-loaded PEOz−hyd−DOX conjugate micelles were prepared by the rotary evaporation method. In order to encapsulate a large amount of DOX, the processing technique of DOX-loaded conjugate micelles was optimized in our preliminary test. Briefly, 25 mg of DOX·HCl and 30 μL of triethylamine (molar ratio = 1:5) were first dissolved in 25 mL of the mixture of chloroform and methanol (2:3, v/v) under stirring in the dark for 24 h. DOX solution was then added to PEOz−hyd−DOX (mass ratio = 1:20) solution in the above mixed solvent followed by evaporation under vacuum at 50 °C to form a thin film. The resultant film was dispersed in 5.0 mL of water at 50 °C and then vortexed for 5 min. The unencapsulated DOX was removed by filtration through a 0.22 μm filter to obtain DOX-loaded PEOz−hyd−DOX conjugate micelle solution.

Physicochemical Characterization of Micelles. The size and size distribution (polydispersity index, PDI) of DOX-loaded conjugate micelles were measured by dynamic light scattering (DLS) (Zetasizer, ZEN 3600, Malvern, UK). All measurements were performed with a scattering angle of 90° at 25 °C. The morphology of DOX-loaded conjugate micelles was visualized by transmission electron microscope (TEM, JEM-1230, JEOL, Japan) with negative stain method as previously reported.[33]

The entrapment efficiency (EE) calculated as the percentage of the amount of the loaded DOX over the original feeding amount of DOX was measured by ultrafiltration centrifugation method using a filtration membrane with MWCO 3500. The amount of the unencapsulated DOX in the collected ultrafiltrate was determined using the HPLC method as described above. The loading content (LC) of micelles was determined by the ratio of the amount of the loaded DOX over the total amount of lyophilized powders of DOX-loaded conjugate micelles.

To evaluate the stability of DOX-loaded conjugate micelles, a sample of the micelle solution in phosphate buffered saline (PBS, pH 7.4) and cell culture medium was stored at 25 °C, respectively. Changes in micelle size were examined as described above.

***In Vitro* Release of DOX from DOX-Loaded Conjugate Micelles.** The *in vitro* release behavior was evaluated as described in the acid degradation of PEOz−hyd−DOX except that 1 mL of PEOz−hyd−DOX solution was replaced by 1 mL of DOX-loaded conjugate micelles solution.

Cell Culture. Human breast cancer cells (MCF-7) were obtained from the Cell Culture Center of the Institute of Basic Medical Sciences, Chinese Academy of Medical Sciences, and Peking Union Medical College. The cells were cultured as previously reported.[46]

***In Vitro* Cytotoxicity Assessment.** Cytotoxicity of various DOX formulations was evaluated by SRB assay.[33] Briefly, MCF-7 cells were seeded at a density of 10^4 cells/well in 96-well plates and cultured for 24 h. After the RPMI-1640 medium was removed, 200 μL of the tested solutions or negative control (FBS-free RPMI-1640) was added to each well and cultured for 24 h. The medium was then removed, the cells were rinsed once with cold PBS, and 200 μL of 10% trichloracetic acid (TCA) was added for fixing at 4 °C for 1 h. Then TCA was removed, and the cells were rinsed with deionized water five times, dried at 37 °C, and stained with 100 μL of 4% (w/v)

DOI: 10.1021/bc5004718
Bioconjugate Chem. 2015, 26, 110−119

SRB in 1% (v/v) acetate solution for 30 min at room temperature. The cells were rinsed with 1% (v/v) acetate solution five times after removing SRB and dried at 37 °C, and then 150 μL of 10 mmol/L Tris was added followed by shaking for 30 min at room temperature. The absorbance of each well was detected at 540 nm with a microplate reader (Bio-Rad model 550, USA). The cytotoxicity of tested samples was evaluated by the relative cell viability, which was the ratio of the absorbance of the tested groups to that of the negative control (100%).

Cellular Uptake and Intracellular Distribution Assay. Confocal microscopy was used to image the uptake of various DOX formulations by MCF-7 cells.[47] Briefly, MCF-7 cells at a density of 10^5/mL were seeded on cover glasses in 24-well plates and cultured at 37 °C in 5% CO_2 for 24 h. After the medium was removed, 1 mL of DOX, PEOz−hyd−DOX, or DOX-loaded conjugate micelle solution in FBS-free 1640 with a final concentration of 10 μg/mL of DOX was added and incubated for predetermined times. After incubation, the medium was removed, and the cells were washed thrice with cold PBS followed by fixing with freshly prepared 4% paraformaldehyde at room temperature for 20 min and then washed thrice with PBS, stained with 500 μL of Hoechst 33258 for 15 min, then rinsed three times with PBS, and finally sealed with glycerin jelly for visualizing the fluorescent images of the cells using confocal laser scanning microscope (CLSM, Leica SP2, Heidelberg, Germany).

***In Vivo* Antitumor Efficacy Evaluation.** MCF-7 cells suspension (0.2 mL, 2×10^6 cells) was injected subcutaneously into the right oxter of the athymic nude mice. When the tumor reached a mean size of approximately 50−100 mm^3, mice were randomly divided into four groups (n = 5) and received intravenous injection of normal saline or various DOX formulations via tail vein at DOX dose of 5 mg/kg at an interval of 2 days for a total of four treatments. The body weight and tumor size were measured every other day throughout the postexposure period. The tumor volume was calculated as (tumor length) × (tumor width)^2/2.

Statistical Analysis. All data were expressed as mean ± standard deviation of independent measurements. Statistical significance of differences between groups was assessed using one-way analysis of variance (ANOVA) or unpaired two-tailed Student's t test. A p-value of 0.05 or less was considered to be statistically significant.

■ ASSOCIATED CONTENT

Supporting Information

Acid/base titration profiles of PEOz-COOH. This material is available free of charge via the Internet at http://pubs.acs.org.

■ AUTHOR INFORMATION

Corresponding Authors

*Phone: 86-10-82801508. E-mail: yanliu@bjmu.edu.cn.
*Phone: 86-10-82801508. E-mail: ll@bjmu.edu.cn.

Notes

The authors declare no competing financial interest.

■ ACKNOWLEDGMENTS

This research was financially supported by the National Natural Science Foundation of China (Grant No. 81172990), the National Key Science Research Program of China (973 Program, 2015CB932100), and the Innovation Team of Ministry of Education (No. BMU20110263).

■ REFERENCES

(1) Cao, N., and Feng, S. S. (2008) Doxorubicin conjugated to D-alpha-tocopheryl polyethylene glycol 1000 succinate (TPGS): Conjugation chemistry, characterization, in vitro and in vivo evaluation. *Biomaterials 29*, 3856−3865.

(2) Greish, K., Sawa, T., Fang, J., Akaike, T., and Maeda, H. (2004) SMA-doxorubicin, a new polymeric micellar drug for effective targeting to solid tumours. *J. Controlled Release 97*, 219−230.

(3) Gabizon, A., Shmeeda, H., and Barenholz, Y. (2003) Pharmacokinetics of pegylated liposomal doxorubicin - Review of animal and human studies. *Clin. Pharmacokinet. 42*, 419−436.

(4) Sun, Y., Zou, W., Bian, S. Q., Huang, Y. H., Tan, Y. F., Liang, J., Fan, Y. J., and Zhang, X. D. (2013) Bioreducible PAA-g-PEG graft micelles with high doxorubicin loading for targeted antitumor effect against mouse breast carcinoma. *Biomaterials 34*, 6818−6828.

(5) Chen, J., Shi, M., Liu, P. M., Ko, A., Zhong, W., Liao, W. J., and Xing, M. M. Q. (2014) Reducible polyamidoamine-magnetic iron oxide self-assembled nanoparticles for doxorubicin delivery. *Biomaterials 35*, 1240−1248.

(6) Upadhyay, K. K., Bhatt, A. N., Mishra, A. K., Dwarakanath, B. S., Jain, S., Schatz, C., Le Meins, J. F., Farooque, A., Chandraiah, G., Jain, A. K., Misra, A., and Lecommandoux, S. (2010) The intracellular drug delivery and anti tumor activity of doxorubicin loaded poly(gamma-benzyl L-glutamate)-b-hyaluronan polymersomes. *Biomaterials 31*, 2882−2892.

(7) Maeda, H., Wu, J., Sawa, T., Matsumura, Y., and Hori, K. (2000) Tumor vascular permeability and the EPR effect in macromolecular therapeutics: A review. *J. Controlled Release 65*, 271−284.

(8) Davis, M. E., Chen, Z., and Shin, D. M. (2008) Nanoparticle therapeutics: An emerging treatment modality for cancer. *Nat. Rev. Drug Discovery 7*, 771−782.

(9) Duncan, R. (2006) Polymer conjugates as anticancer nanomedicines. *Nat. Rev. Cancer 6*, 688−701.

(10) Chytil, P., Etrych, T., Koňák, Č., Šírová, M., Mrkvan, T., Říhová, B., and Ulbrich, K. (2006) Properties of HPMA copolymer−doxorubicin conjugates with pH-controlled activation: Effect of polymer chain modification. *J. Controlled Release 115*, 26−36.

(11) Jiang, T., Li, Y. M., Lv, Y., Cheng, Y. J., He, F., and Zhuo, R. X. (2013) Amphiphilic polycarbonate conjugates of doxorubicin with pH-sensitive hydrazone linker for controlled release. *Colloids Surf., B 111*, 542−548.

(12) Li, H. N., Bian, S. Q., Huang, Y. H., Liang, J., Fan, Y. J., and Zhang, X. D. (2014) High drug loading pH-sensitive pullulan-DOX conjugate nanoparticles for hepatic targeting. *J. Biomed. Mater. Res., Part A 102*, 150−159.

(13) Chtryt, V., and Ulbrich, K. (2001) Conjugate of doxorubicin with a thermosensitive polymer drug carrier. *J. Bioact. Compat. Polym. 16*, 427−440.

(14) Hopewell, J. W., Duncan, R., Wilding, D., and Chakrabarti, K. (2001) Preclinical evaluation of the cardiotoxicity of PK2: A novel HPMA copolymer-doxorubicin-galactosamine conjugate antitumour agent. *Hum. Exp. Toxicol. 20*, 461−470.

(15) Lu, D. X., Liang, J., Fan, Y. J., Gu, Z. W., and Zhang, X. D. (2010) In vivo evaluation of a pH-sensitive pullulan-doxorubicin conjugate. *Adv. Eng. Mater. 12*, B496−B503.

(16) Yang, R. L., Zhang, S. A., Kong, D. L., Gao, X. L., Zhao, Y. J., and Wang, Z. (2012) Biodegradable polymer-curcumin conjugate micelles enhance the loading and delivery of low-potency curcumin. *Pharm. Res. 29*, 3512−3525.

(17) Cui, C., Xue, Y. N., Wu, M., Zhang, Y., Yu, P., Liu, L., Zhuo, R. X., and Huang, S. W. (2013) Cellular uptake, intracellular trafficking, and antitumor efficacy of doxorubicin-loaded reduction-sensitive micelles. *Biomaterials 34*, 3858−3869.

(18) Torchilin, V. (2009) Multifunctional and stimuli-sensitive pharmaceutical nanocarriers. *Eur. J. Pharm. Biopharm. 71*, 431−444.

DOI: 10.1021/bc5004718
Bioconjugate Chem. 2015, 26, 110−119

(19) Bareford, L. A., and Swaan, P. W. (2007) Endocytic mechanisms for targeted drug delivery. *Adv. Drug Delivery Rev. 59*, 748−758.
(20) Rong, T., and Jianjun, C. (2007) Anticancer polymeric nanomedicines. *Polym. Rev. 47*, 345−381.
(21) Guo, X., Shi, C. L., Wang, J., Di, S. B., and Zhou, S. B. (2013) pH-triggered intracellular release from actively targeting polymer micelles. *Biomaterials 34*, 4544−4554.
(22) Martin, G. R., and Jain, R. K. (1994) Noninvasine measurement of interstitial pH profiles in normal and neoplastic tissue using fluorescence ratio imaging microscopy. *Cancer Res. 54*, 5670−5674.
(23) Hu, X. L., Wang, R., Yue, J., Liu, S., Xie, Z. G., and Jing, X. B. (2012) Targeting and anti-tumor effect of folic acid-labeled polymer-doxorubicin conjugates with pH-sensitive hydrazone linker. *J. Mater. Chem. 22*, 13303−13310.
(24) Van Kuringen, H. P., Lenoir, J., Adriaens, E., Bender, J., De Geest, B. G., and Hoogenboom, R. (2012) Partial hydrolysis of poly(2-ethyl-2-oxazoline) and potential implications for biomedical applications? *Macromol. Biosci. 12*, 1114−1123.
(25) Bauer, M., Lautenschlaeger, C., Kempe, K., Tauhardt, L., Schubert, U. S., and Fischer, D. (2012) Poly(2-ethyl-2-oxazoline) as alternative for the stealth polymer poly(ethylene glycol): comparison of in vitro cytotoxicity and hemocompatibility. *Macromol. Biosci. 12*, 986−998.
(26) Luxenhofer, R., Han, Y., Schulz, A., Tong, J., He, Z., Kabanov, A. V., and Jordan, R. (2012) Poly(2-oxazoline)s as polymer therapeutics. *Macromol. Rapid Commun. 33*, 1613−1631.
(27) Sedlacek, O., Monnery, B. D., Filippov, S. K., Hoogenboom, R., and Hruby, M. (2012) Poly(2-oxazoline)s−are they more advantageous for biomedical applications than other polymers? *Macromol. Rapid Commun. 33*, 1648−1662.
(28) Wang, X., Li, X., Li, Y., Zhou, Y., Fan, C., Li, W., Ma, S., Fan, Y., Huang, Y., Li, N., and Liu, Y. (2011) Synthesis, characterization and biocompatibility of poly(2-ethyl-2-oxazoline)-poly(D,L-lactide)-poly-(2-ethyl-2-oxazoline) hydrogels. *Acta Biomater. 7*, 4149−4159.
(29) Wang, C. H., and Hsiue, G. H. (2003) New amphiphilic poly(2-ethyl-2-oxazoline)/poly(L-lactide) triblock copolymers. *Biomacromolecules 4*, 1487−1490.
(30) Wang, C. H., and Hsiue, G. H. (2002) Synthesis and characterization of temperature- and pH-sensitive hydrogels based on poly(2-ethyl-2-oxazoline) and poly(D,L-lactide). *J. Polym. Sci., Part A: Polym. Chem. 40*, 1112−1121.
(31) Gao, Y. j., Li, Y. F., Li, Y. S., Yuan, L., Zhou, Y. X., Li, J. W., Zhao, L., Zhang, C., Li, X. Y., and Liu, Y. (2015) PSMA-mediated endosome escape-accelerating polymeric micelles for targeted therapy of prostate cancer and the real time tracing of their intracellular trafficking. *Nanoscale 7*, 597−612.
(32) Colombo, P.-E., Boustta, M., Poujol, S., Pinguet, F., Rouanet, P., Bressolle, F., and Vert, M. (2007) Biodistribution of doxorubicin-alkylated poly(l-lysine citramide imide) conjugates in an experimental model of peritoneal carcinomatosis after intraperitoneal administration. *Eur. J. Pharm. Sci. 31*, 43−52.
(33) Li, N., Li, X.-R., Zhou, Y.-X., Li, W.-J., Zhao, Y., Ma, S.-J., Li, J.-W., Gao, Y.-J., Liu, Y., Wang, X.-L., and Yin, D.-D. (2012) The use of polyion complex micelles to enhance the oral delivery of salmon calcitonin and transport mechanism across the intestinal epithelial barrier. *Biomaterials 33*, 8881−8892.
(34) Pan, X., Yu, S., Yao, P., and Shao, Z. (2007) Self-assembly of beta-casein and lysozyme. *J. Colloid Interface Sci. 316*, 405−412.
(35) Wenchuan, S., Kui, L., Chengyuan, Z., Gang, W., Yanyan, G., Li, L., Bin, H., and Zhongwei, G. (2013) The potential of self-assembled, pH-responsive nanoparticles of mPEGylated peptide dendron-doxorubicin conjugates for cancer therapy. *Biomaterials 34*, 1613−1623.
(36) Li, C., and Wallace, S. (2008) Polymer-drug conjugates: Recent development in clinical oncology. *Adv. Drug Delivery Rev. 60*, 886−898.
(37) Zalipsky, S., Hansen, C. B., Oaks, J. M., and Allen, T. M. (1996) Evaluation of blood clearance rates and biodistribution of poly(2-oxazoline)-grafted liposomes. *J. Pharm. Sci. 85*, 133−137.
(38) Chen, R. Z., N, X., Qi, H., and Li, H. (1996) Cationic ring-open polymerization of 2-ethyl-2-oxazoline and characterization of polymer. *J. Nanjing Univ. Chem. Technol. 18*, 9−14.
(39) Verbraeken, B., Lava, K., and Hoogenboom, R. (2014) Poly(2-oxazoline)s. *Encyclopedia of Polymer Science and Technology*; Wiley. doi: 10.1002/0471440264.pst626.
(40) Sanson, C., S, C., Le Meins, J. F., Soum, A., Thevenot, J., Garanger, E., and Lecommandoux, S. (2010) A simple method to achieve high doxorubicin loading in biodegradable polymersomes. *J. Controlled Release 147*, 428−435.
(41) Kim, D., Gao, Z. G., Lee, E. S., and Bae, Y. H. (2009) In vivo evaluation of doxorubicin-loaded polymeric micelles targeting folate receptors and early endosomal pH in drug-resistant ovarian cancer. *Mol. Pharmaceutics 6*, 1353−1362.
(42) Wang, C.-H., Wang, C.-H., and Hsiue, G.-H. (2005) Polymeric micelles with a pH-responsive structure as intracellular drug carriers. *J. Controlled Release 108*, 140−149.
(43) Liang, Q.-F., Liu, J.-J., and Chen, J. (2011) Sandwich structure of a ruthenium porphyrin and an amino acid hydrazide for probing molecular chirality by circular dichroism. *Tetrahedron Lett. 52*, 3987−3991.
(44) Briner, K., Collado, I., Fisher, M. J., García-Paredes, C., Husain, S., Kuklish, S. L., Mateo, A. I., O'Brien, T. P., Ornstein, P. L., Zgombick, J., and de Frutos, Ó. (2006) Privileged structure based ligands for melanocortin-4 receptors—aliphatic piperazine derivatives. *Bioorg. Med. Chem. Lett. 16*, 3449−3453.
(45) Hruby, M., Konak, C., and Ulbrich, K. (2005) Polymeric micellar pH-sensitive drug delivery system for doxorubicin. *J. Controlled Release 103*, 137−148.
(46) Li, X. R., Li, P. Z., Zhang, Y. H., Zhou, Y. X., Chen, X. W., Huang, Y. Q., and Liu, Y. (2010) Novel mixed polymeric micelles for enhancing delivery of anticancer drug and overcoming multidrug resistance in tumor cell lines simultaneously. *Pharm. Res. 27*, 1498−1511.
(47) Duan, X., Xiao, J., Yin, Q., Zhang, Z., Yu, H., Mao, S., and Li, Y. (2013) Smart pH-sensitive and temporal-controlled polymeric micelles for effective combination therapy of doxorubicin and disulfiram. *ACS Nano 7*, 5858−5869.

DOI: 10.1021/bc5004718
Bioconjugate Chem. 2015, 26, 110−119